Mol Cell Biochem (2007) 306:123–132
DOI 10.1007/s11010-007-9561-z

RNA interference in human foreskin fibroblasts within the three-dimensional collagen matrix

Mark A. Carlson · Amy K. Prall · Jeremiah J. Gums

Received: 17 March 2007 / Accepted: 12 July 2007 / Published online: 27 July 2007

Abstract The technique of RNA interference (RNAi) was trialed in primary human foreskin fibroblasts, both in monolayer culture and in the fibroblast-populated collagen matrix. Knockdown of lamin A/C, p53, and FAK was possible with low-confluency (<50%) monolayer fibroblasts, a transfection vehicle concentration of 1%, and an siRNA concentration of 25–50 nM. Knockdown also was possible in the collagen matrix using similar reagent concentrations and a cellular density of one million fibroblasts per ml of matrix. Optimization of transfection conditions appeared to be important to increase knockdown efficiency. Consistent with prediction, knockdown of FAK induced apoptosis in the fibroblast-populated collagen matrix.

Keywords RNA interference · Fibroblast · Collagen · Extracellular matrix · Focal adhesion kinase · p53

Abbreviations

DAPI	4′,6-Diamidino-2-phenylindole
FAK	Focal adhesion kinase
FBS	Fetal bovine serum
DMEM	Dulbecco's modified Eagle's medium
PBS	Phosphate buffered saline
PI	Propidium iodide
RNAi	RNA interference
SDS-PAGE	Sodium dodecyl sulfate polyacrylamide gel electrophoresis
ShRNA	Short hairpin RNA duplex
SiRNA	Short interfering RNA duplex
TUNEL	Terminal deoxynucleotidyltransferase-mediated dUTP nick-end labeling

M. A. Carlson (✉) · A. K. Prall · J. J. Gums
Department of Surgery, VA Nebraska-Western Iowa Health Care System, Surgery 112, VA Medical Center, 4101 Woolworth Avenue, Omaha, NE 68105, USA
e-mail: macarlso@unmc.edu

M. A. Carlson · A. K. Prall · J. J. Gums
University of Nebraska Medical Center, Omaha, NE, USA

Introduction

RNA interference (RNAi) of primary cells is possible but typically more difficult than with transformed cell lines [1, 2]; this also is the case with gene transfer [3]. The advantages of working with primary cells include the fact that signaling transduction pathways are intact; this is particularly relevant when dealing with the p53 network, which often becomes dysfunctional in the process of cell immortalization. If an investigator is dealing with the fibroblast, then further of in vivo relevance may be obtained by culturing the cells within a three-dimensional collagen matrix [4–6]. This system better replicates in vivo conditions than monolayer culture [7].

While a three-dimensional collagen matrix may produce more physiologic culture conditions, it also presents a number of difficulties for the investigator, such as an abundance of collagen that adsorbs reagent molecules, confounds assays, and makes separation/purification sometimes impossible. Despite these drawbacks, the advantages of working with primary cells in a physiologic matrix was attractive enough for us to attempt RNAi of the fibroblasts embedded in the collagen matrix. This work should provide another inroad to study the relevance of p53 and other proteins in fibroblast survival and proliferation

in the three-dimensional collagen matrix, an area which has direct relevance to wound healing [8, 9].

Materials and methods

Reagents

FBS, goat serum, DMEM, Opti-MEM®, Antibiotic/Antimycotic solution, and Fungizone were from Invitrogen; FAK antibody (C-20) was from Santa Cruz; p53 antibody (Ab-7) was from Oncogene; lamin A/C antibody (clone 14) was from BD Transduction Laboratories; α-tubulin antibody (clone DM 1A) was from Sigma; GAPDH antibody (rabbit polyclonal) was from Abcam; secondary antibodies (Alexa Fluor®) and phalloidin derivatives were from Molecular Probes; Type I bovine collagen (PureCol™) was from Inamed; siRNA transfection vehicle (*Trans*IT-TKO® Transfection Reagent) was from Mirus®; siRNA, including pooled siRNA (*SMART*pool), and fluorescently-labeled RNA (si*GLO*™), were from Dharmacon (sequences are available from the corresponding author); TUNEL kits (*In Situ* Cell Death Detection Kit, Fluorescein) were from Roche; and miscellaneous chemicals/reagents were purchased from Sigma or Invitrogen.

Cell culture

The use of primary dermal fibroblasts derived from human tissue was approved by our Institutional Review Board. Fibroblasts were cultured from explants of neonatal foreskin as previously described [10]. Cells were maintained in T75 flasks with growth medium (defined as DMEM supplemented with 20 mM HEPES, 44 mM sodium bicarbonate, 1% Antibiotic/Antimycotic Solution, 1.5 μg/ml Fungizone, and 10% FBS; final pH = 7.2). The fibroblasts were stored at P7 in liquid N_2; to perform an experiment; a vial of P7 cells was thawed, plated, and split according to a rigid schedule; virtually all experiments were performed on P9 cells from the same donor.

Fibroblast-populated collagen matrix

The collagen matrix model was utilized as previously described [10, 11]. Final parameters were: matrix volume = 0.2 ml; matrix diameter = 12 mm; collagen concentration = 1.5 mg/ml; and cell concentration = 1.0×10^6 per ml. Matrices were made in groups of 18 (i.e., three rows of a 24-well plate), and incubated in the attached state in growth medium (supplemented with 50 μg/ml ascorbic acid) for typically 72 h prior to the initiation of an experiment.

TUNEL

The TUNEL assay was performed as previously described on cytospin preparations of fibroblasts retrieved from the collagen matrix after digestion of the matrix with a trypsin/collagenase sequence [10, 11].

Transfections

The transfection protocol was adopted from the Mirus® web site (http://www.genetransfer.com/products/techresources, protocol# ML015; revised 11/15/05). Monolayer fibroblasts in 35 mm wells (i.e., 6-well plates) were cultured at low density in growth medium for 24 h, as described in the figure legends. For a typical 6-well transfection, serum-free transfection media (Opti-MEM®, 1.5 ml) was combined with transfection vehicle (*Trans*IT-TKO®, 180 μl) and incubated for 10 min at 22°C; siRNA stock (typically 20 μM) or buffer then was added (45 μl aliquot), and this complex mixture was incubated at 22°C for another 10 min. The growth medium in all wells then was replaced with 2.71 ml of fresh growth medium, and complex mixture (285 μl) was added to each well to make a final transfection volume of 3 ml. The final concentrations of the transfection vehicle and siRNA in this example were thus approximately 1% and 50 nM, respectively. The plate was incubated for 24 h at 37°C, and then the transfection medium was changed to regular growth medium; the growth medium subsequently was exchanged every 48 h until completion of the experiment. Collagen matrices were transfected in a similar fashion, but the matrix incubation period prior to addition of the transfection medium was 72 h, and the transfection volume in each well of the 24-well plate was 1 ml.

Quantitative immunofluorescence

Cytospin preparations (one cell-layer thick) of fibroblasts were fixed in 70% ethanol at 22°C for 15 min, permeabilized with 0.5% Triton® X-100 in PBS at 22°C for 30 min, rinsed with PBS, and then incubated in blocking buffer (2% goat serum in PBS) at 22°C for 30 min. The slides then were incubated in primary antibody (typically diluted 1:100 with blocking buffer) overnight at 4°C. After this, the slides were rinsed in PBS, and incubated with fluorescently-labeled secondary antibody (diluted 1:200 in blocking buffer) at 22°C for 1 h. The slides then were rinsed again with PBS, counterstained with PI (5 μg/ml with 20 μg/ml DNAse-free RNAse in PBS) or DAPI (1 μg/ml in PBS) for 15 min at 22°C and, after a final rinsing with PBS, were coverslipped (#1 glass) with Immu-Mount™ (Thermo Scientific). The slides were viewed with fluorescent microscopy; digital images (1600 × 1200

pixels) of at least five microscopic fields (field dimension with the 20× objective = 153 × 115 μm) per slide subsequently were captured. Using ImageJ software (http://www.rsb.info.nih.gov/ij/), each image was converted to an 8-bit black-and white-format, and thresholded at a grey value of 108 (where 0 = pure black, or no signal; and 256 = pure white, or strongest signal) in order to eliminate background fluorescence. The number of pixels registering at or above the threshold value (the "positive" pixels) was divided by the number of counterstained nuclei (typically ~150) in that image, thus yielding an antigen index defined as the number of positive pixels per nuclei. In other words, the antigen index was the amount of antigen signal in a given image normalized to the number of nuclei. The efficiency of knockdown was calculated after determining the antigen index with and without siRNA treatment.

Immunoblotting and densitometry

These procedures were performed as previously described [10]. Except where indicated, each immunoblot lane was loaded with 10 μg of cellular protein. Protein concentration in monolayer lysates was determined with a Bio-Rad assay as previously described [12]. Since protein assays are not precise in lysates of the fibroblast-populated collagen matrix, lane loading for immunoblots involving these lysates was based on cell number and corroborated with an immunoblot loading control, such as GAPDH or α-tubulin [12].

Statistical analysis and image manipulation

Numerical data were expressed as mean ± SD. Groups of unpaired data were compared with ANOVA, using a level of significance of $P < 0.05$. Some of the microscopic images were contrast-enhanced with Photoshop®, as indicated in the figure legends. If contrast enhancement was done, it was performed equally among all images in a group. None of the images were "cleaned up," i.e., there was no deletion of smudges, artifact, noise, etc.

Results

Effect of the transfection vehicle on fibroblast biology

The transfection of siRNA into cells typically involves a lipid-based reagent. We chose one of the proprietary formulations that seemed to work reasonably well in our model, the fibroblast-populated collagen matrix. Some of the essential behavior of this model [4, 5] is illustrated in Fig. 1A. Fibroblasts in a three-dimensional collagen (type I) matrix will, in the presence of serum, contract, and organize the matrix. The matrix on the left in Fig. 1A is attached to the tissue culture plastic, which results in the mechanical tension ("preload") in the horizontal plane. If the matrix is detached from the culture dish, then the matrix contracts as shown on the right in Fig. 1A. An interesting difference between these two states is that the fibroblasts in the attached matrix proliferate, while those in the released matrix become quiescent, with a subpopulation undergoing apoptosis [5].

We wanted to determine if the transfection vehicle was toxic to fibroblasts, so we measured the effect of the vehicle on matrix contraction, as shown in Fig. 1B, C. Transfection vehicle (up to 4% for 24 h prior to matrix release) did not have a significant effect on contraction. We did observe an effect on monolayer fibroblast morphology when the vehicle was applied at the ≥2.5% (Fig. 1D). The cells treated with this vehicle concentration assumed a thinner, more spindle-shaped appearance, and there also was a greater amount of debris floating in the medium. Since it was not clear what was going at this vehicle concentration, we elected to utilize 1% vehicle (also recommended by the manufacturer). We next treated the fibroblast-populated collagen matrix with 1% vehicle for 24 h prior to performing the TUNEL assay on cytospin preparations in order to determine the effect on this important assay (see Fig. 1). The addition of the vehicle did not effect the basal apoptotic rate, which was 1–2%. Of note, we have performed simultaneous immunostaining for activated caspase-3 and TUNEL on similar specimens, and have attained >75% concordance between these two assays in identifying apoptotic cells (data not shown), which is in agreement with the results of others [13–15].

Transfection efficiency using a labeled nonfunctional short RNA duplex in the fibroblast-populated collagen matrix

We next wanted to determine if 1% vehicle could transport a short RNA duplex into the fibroblasts. For this purpose a commercially-available short RNA duplex labeled with a fluorescent tag (rhodamine filter), and which purportedly has no known target effects, was transfected into attached matrices which were then imaged intact with confocal microscopy. As shown in Fig. 2, transfection with vehicle only resulted in no fluorescence, while the matrix transfected with the labeled RNA duplex demonstrated abundant uptake. On close examination of these images there appears to be the presence of red fluorescence not associated with intracellular space in the RNA-treated matrix (see arrowheads in inset a). Most of the true uptake was associated with the cytoplasm, however, and not the nucleus (see inset b). Another interesting finding of these in situ images of the three-dimensional matrix is that there

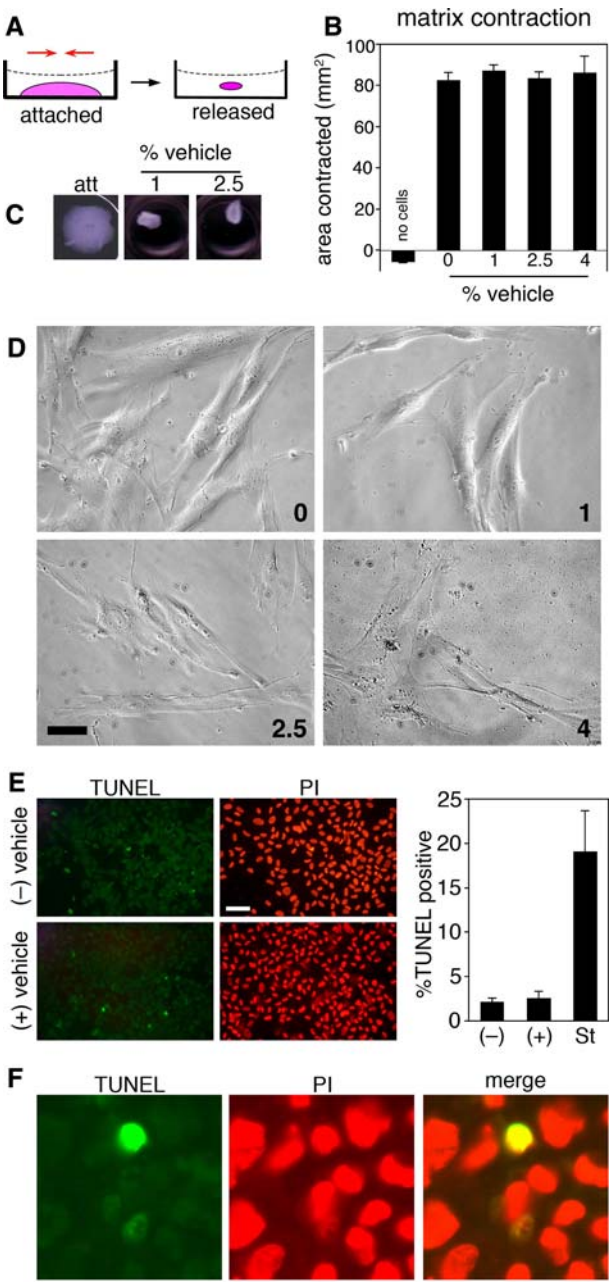

◀ **Fig. 1** Transfection vehicle toxicity. (**A**) Stressed matrix contraction (side view). Fibroblast-populated collagen matrices attached to a culture plate and incubated with growth medium develop horizontal cell-dependent tension. Release of this matrix from the plate results in contraction. (**B**) Stressed matrix contraction (1 h after release) in the presence of zero to 4% transfection vehicle; mean of six areas ± SD; taller bar = greater contraction. (**C**) Overhead views of an attached matrix (*att*), and 1 h after release with vehicle. (**D**) Phase images (contrast-enhanced) of fibroblasts cultured 24 h in growth medium/lipid transfection vehicle (% in lower right); bar = 50 μm. (**E**) Effect of lipid transfection vehicle on fibroblast apoptosis in three-dimensional culture. Attached matrices were cultured 3 days in growth medium prior to the vehicle (1%) for another 24 h. TUNEL (with PI counterstain) was performed on cytospin preparations, and the TUNEL index (mean ± SD, three preps) was plotted at right. TUNEL images underwent equal contrast enhancement. Matrices treated with 1 μM staurosporine (St) × 4 h used as a positive control [11]. (**F**) Higher power views of a typical TUNEL-positive nuclei from a cytospin prep with PI counterstaining with image merging

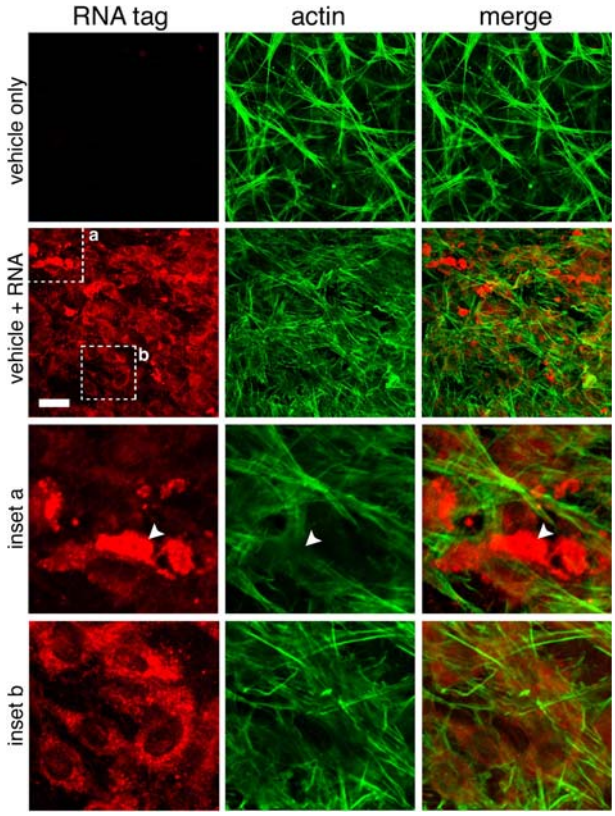

Fig. 2 Transfection of human fibroblasts embedded in a three-dimensional collagen matrix with a labeled, nonfunctional double-stranded RNA oligomer. Anchored matrices were incubated in growth medium for 3 days prior to transfection with 1% vehicle ± 25 nM of the fluorescently-labeled RNA duplex. Intact matrices subsequently were fixed in 95% ethanol one day post-transfection, counterstained with phalloidin-AF488, and examined with confocal microscopy (Zeiss LSM 410). Bar = 50 μm. Arrowheads of inset *a* indicate brightly fluorescent material which does not appear to be associated with intracellular space (i.e., a false signal). Inset *b* demonstrates true signal. Images underwent equal contrast enhancement in Photoshop to increase clarity

appears to be an effect of the labeled RNA duplex on the actin cytoskeleton, which was counterstained with a phalloidin reagent (green fluorescence). The cells in the matrix treated with vehicle only were thin, elongate, and densely colored with the stain; the cells treated with vehicle and the tagged RNA, however, were more flattened and translucent. The meaning and relevance of this observation is not clear. The more important finding in Fig. 2, however, was that the transfection efficiency of the tagged RNA (25 nM) in the fibroblast-populated collagen matrix using 1% vehicle was high–the vast majority of cells (>90%) had

some degree of tracer uptake. This was the rationale for the initial choice of 25 nM siRNA in subsequent experiments.

RNAi of lamin A/C in 293T cells and fibroblasts, and the effect of pre-transfection trypsinization

We needed a positive RNAi control in a cell line that would be relatively easy to transfect, such as large T antigen-transformed human embryonic kidney (293T) cells. RNAi of lamin A/C in 293T cells is shown in Fig. 3A; the knockdown of this intermediate filament protein, as determined with quantitative immunhistochemistry on cytospin preparations, was virtually complete (99.2 ± 0.3%). For comparison, RNAi of lamin A/C in the fibroblast-populated collagen matrix under similar transfection conditions was partial (55.5 ± 11.7%; Fig. 3A).

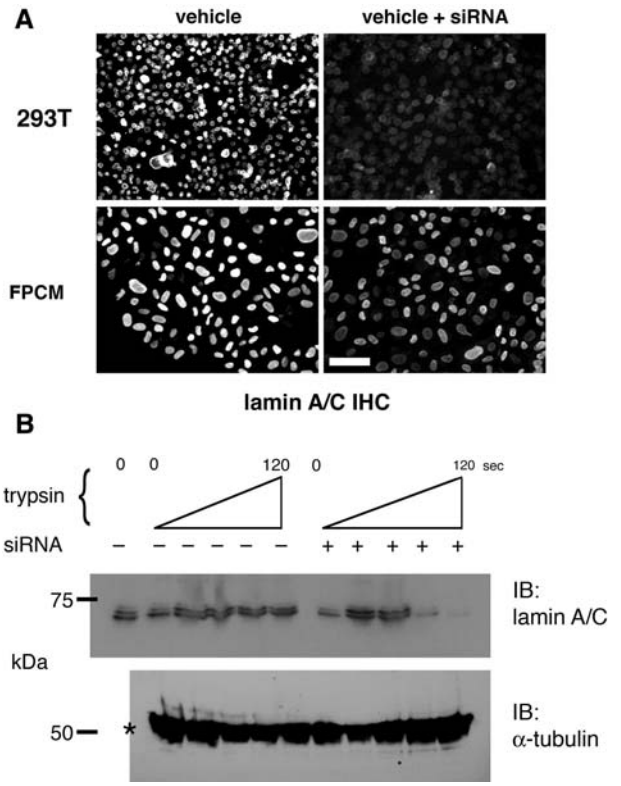

Fig. 3 RNAi of lamin A/C in 293T cells and human foreskin fibroblasts. (**A**) Monolayer 293T cells (35 mm dishes, 60–80% confluent) and attached fibroblast-populated collagen matrices (FPCM; 72 h old) were transfected with vehicle ± lamin A/C siRNA (25 nM, single oligomer), and cytospin preparations then underwent lamin A/C immunohistochemistry 48 h post-transfection. Bar = 50 μm. (**B**) Monolayer fibroblasts (30,000 per 35 mm dish) were cultured for 24 h in growth medium, and then underwent brief trypsinization (0–120 s) prior to transfection with vehicle ± lamin A/C siRNA (10 nM, single oligomer). Lysates were made 48 h post-transfection and immunoblotted (10 μg per lane) for lamin A/C and α-tubulin. All images raw/nonenhanced. *Asterisk indicates that the sample was lost, and nothing was loaded for this lane (i.e., the tubulin blot for the -trypsin/-siRNA control)

Interestingly, there appears to have been a range of lamin knockdown within individual fibroblasts, from minimal to near-complete. A range of transfection conditions (i.e., different combinations of siRNA and vehicle concentration) were tested in the collagen matrix (data not shown) in order to optimize the knockdown efficiency, but none were any better than the conditions given in Fig. 3A (25 nM siRNA and 1% vehicle).

In an attempt to increase the lamin A/C knockdown efficiency in human fibroblasts, we subjected monolayer cells to brief trypsinization [16] prior to adding the transfection medium (see Fig. 3B). With ~60 s of trypsinization, an increase in the lamin knockdown efficiency (as determined with immunoblotting) was noted. This degree of trypsinization corresponded to partial "rounding" of the elongated, adherent fibroblasts on the culture plate (data not shown). We then applied various courses of trypsinization to the fibroblast-populated collagen matrix to see whether this adjunct could augment knockdown efficiency in the three-dimensional culture system. Unfortunately, no effect was seen (data not shown); furthermore, an untoward outcome of this pretreatment was gradual disintegration of the matrix over the ensuing 2–3 days.

The effect of cell plating density on p53 RNAi in monolayer fibroblasts

We wanted to determine if knockdown of p53 would be feasible in foreskin fibroblasts, so that we could test the role of p53 in regulation of survival in the fibroblast-populated collagen matrix [17]. p53 RNAi was attempted in more tractable monolayer system first; the effect of fibroblast plating density on subsequent p53 knockdown is shown in Fig. 4. The approximate confluency that the lowest and highest plating number produced after 24 h of culture is shown in the phase images at the bottom of this figure. The SDS-PAGE gel lanes in Fig. 4 were loaded with equal volumes of lysate in order to determine if the relative amount of cellular protein was different among the various plating conditions. The bands of the GAPDH loading control suggested that after 4 or 6 days of monolayer culture (3 or 5 days after transfection, respectively), there was not a large difference in the amount of protein in each lysate, as there might have been after 1 day of culture (see phase images). The p53 immunoblots of the vehicle-only transfected matrices tended to be somewhat "dirty," with an appropriate band seen at ~53 kDa, but also with an accompanying smear. The presence of smearing was not limited to p53 Westerns, but was variably (and unpredictably) present in many of the collagen matrix Westerns. This may be related to an unknown amount of solubilized extracellular matrix retained in the supernatant of a collagen matrix lysate. The vehicle-only p53 blot also had a

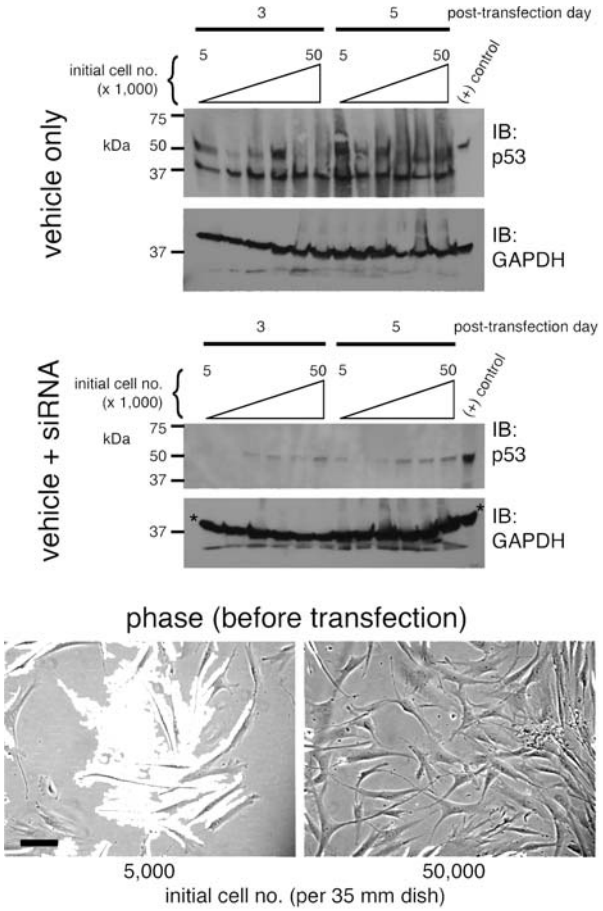

Fig. 4 RNAi of p53 in monolayer human foreskin fibroblasts. Monolayer cells were cultured in growth medium inside 35 mm dishes (i.e., 6-well plates) with an initial plating density of 5,000–50,000 cell/dish; after 24 h, the cells were transfected with 1% vehicle ± p53 siRNA (50 nM, pooled oligomers). Monolayer lysates (equal volumes; see text for justification) were immunoblotted for both p53 and GAPDH at 3 and 5 days post-transfection. Identity of the band near 37 kDa in the p53 blot (vehicle only samples) is unknown; the identity of the GAPDH band in the lower set of blots is indicated with asterisks (*). Phase images are of monolayer fibroblasts just prior to transfection (contrast-enhanced in Photoshop)

constant band of unknown identity at ~37 kDa. There was a convincing (but not complete) knockdown of both p53 and the 37 kDa band at both 3 and 5 days post-transfection with pooled siRNA against p53. There does appear to be a trend of more efficient knockdown at the lower plating densities, but this observation was consistent in no more than half of the experiments of this type. Unfortunately, our efforts to date to knockdown p53 directly in the fibroblast-populated collagen matrix have been erratic (data not shown).

RNAi of FAK in monolayer fibroblasts and the fibroblast-populated collagen matrix

In addition to p53, focal adhesion kinase (FAK) also has been shown to regulate survival in cultured fibroblasts [17, 18] and the collagen matrix [19]. RNA interference of FAK has been utilized in fibroblast cell lines [20], but apparently not in primary dermal fibroblasts. We treated subconfluent plates of fibroblasts with vehicle ± siRNA against FAK, and found that the immunoblot signal for FAK decreased progressively out to 6 days post-transfection (Fig. 5A). Similar to Fig. 4, the lanes of electrophoretic gel

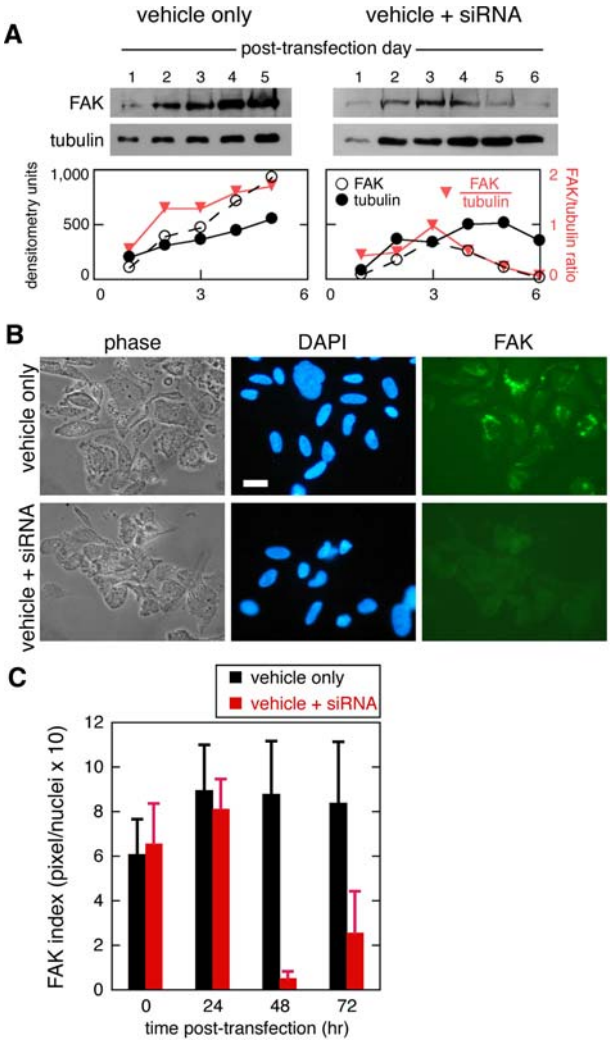

Fig. 5 RNAi of FAK in human fibroblasts. (**A**) Cells cultured in 35 mm plates (2×10^4 cell/well) 24 h with growth medium, then transfected with 1% vehicle ± FAK siRNA (50 nM, single oligomer). Lysates (equal volumes; see text) blotted for FAK and α-tubulin on indicated days. Densitometry: individual bands (*black symbols*) and the expression of FAK with respect to α-tubulin (*red triangles*). (**B**) Fibroblasts embedded in collagen matrices cultured in growth medium 48 h then transfected with 1% vehicle ± 50 nM siRNA (FAK, pooled oligomers). Cytospin preps at 0–3 days immunostained for FAK (day 3 images are shown). Bar = 20 μm. FAK images are nonenhanced; phase and DAPI images contrast-enhanced. (**C**) Quantitative immunohistochemistry (see Methods) for FAK in cells isolated from collagen matrices which had been treated ±50 nM siRNA (FAK, pooled oligomers). Each bar represents the mean ± SD of ≥5 microscopic fields, an example of which is given in (**B**)

of Fig. 5A were loaded with an equal volume of lysate in order to reflect the concentration of protein in the lysate (which would be an indicator of cell number per plate). The gradual increase in the intensity of the loading control (α-tubulin) in Fig. 5A is secondary to an increasing cell number (i.e., cell division) in the monolayer plates. Fibroblast-populated collagen matrices then were transfected in a similar fashion, and evaluated with FAK immunofluorescence (Fig. 5B). Preliminary experiments (data not shown) confirmed that an siRNA concentration of 25 nM was optimal. There was reasonably strong knockdown (70–90%) of FAK at 2–3 days post-transfection. FAK RNAi in the fibroblast-populated collagen matrix was confirmed in other experiments with immunoblotting (see below).

The effect of FAK knockdown on fibroblast survival in the collagen matrix

The predicted effect of FAK knockdown in primary dermal fibroblasts would be upregulation of apoptosis, as implied above. We transfected fibroblast-populated collagen matrices as done in Fig. 5, and then performed the TUNEL assay on cytospin preparations, along with FAK immunoblotting on lysates of intact matrices (Fig. 6). The increase in TUNEL positivity with the siRNA-treated matrices was obvious (Fig. 6A), suggesting that FAK knockdown was inhibiting survival; this was consistent with previously published results [17–19]. The simultaneous Western blots for FAK (Fig. 6B) are subtle, but do suggest a decrease of FAK in the siRNA-treated lanes. Quantification of the TUNEL assay is shown in Fig. 6C; TUNEL positivity (i.e., % apoptotic) increased steadily out to 4 days post-transfection. Interestingly, there also appeared to be a negative effect of the transfection vehicle on fibroblasts survival, which was most apparent on post-transfection day 3. This finding might have accounted for a small fraction of the apoptosis induced by siRNA transfection; this finding also was a reminder that lipid-based transfection vehicles can have independent effects.

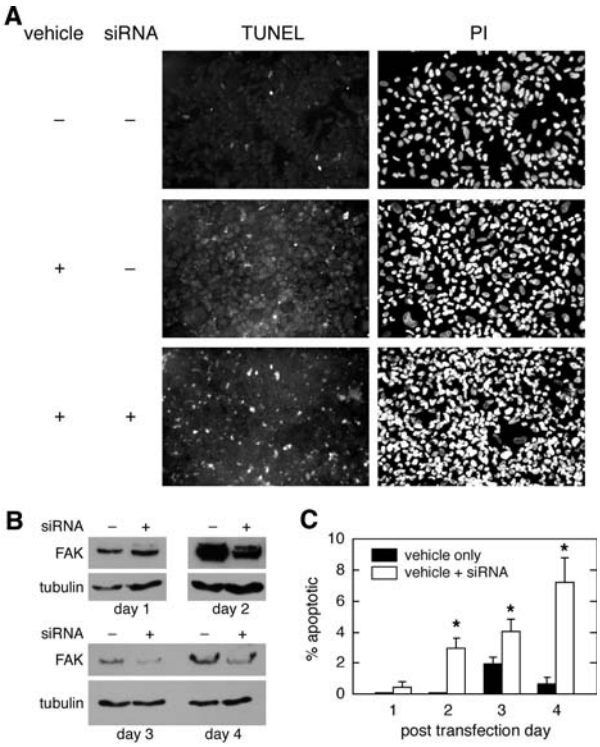

Fig. 6 Effect of FAK RNAi on fibroblast survival in the collagen matrix. Attached matrices were incubated in growth medium for 3 days prior to transfection with 1% vehicle ± FAK siRNA (50 nM, pooled oligomers), and then matrices were analyzed 1–4 days post-transfection. (**A**) The TUNEL assay was performed on cytospin preparations of the matrices; shown are sample images (raw, nonenhanced) from post-transfection day 4 (quantification shown in panel C). (**B**) Immunoblotting for FAK and α-tubulin was performed on dounced and spun matrix lysates. (**C**) Quantification of TUNEL results (see Methods). Each bar represent the mean ± SD of ≥5 microscopic fields, an example of which is given in (**A**)

Discussion

A noteworthy aspect of the above data which was not stressed was the relative inconsistency of the results. Often an RNAi experiment would not demonstrate any target knockdown on the first attempt, but this did not necessarily indicate a true negative finding. It has been our experience with primary foreskin fibroblasts that an experiment should not be branded as "negative" (i.e., not exposing a difference) until three consecutive negative results are obtained. If an RNAi experiment did yield knockdown during the initial three attempts, then the positive result would have to be repeated at least once—and in actual fact was repeated two or three times more. A curious and sometimes confounding observation with this model is that two experiments performed identically on different days can have markedly different results [21]. We have taken numerous measures to limit this problem, such as regimenting the cell culture protocol in terms of days in culture, number of cells per flask, etc. with no diminish of this problem. The only conclusion that we can make at this point is that there is some unidentified mechanism in our system which produces variable RNAi results; in the collagen matrix system, we suspect that the variability may be secondary to an unpredictable tendency of the matrix to sequester the reagents.

One potential source of variability which was limited in this manuscript was the genetic variability of the fibroblasts strain. Virtually all of the foreskin fibroblasts utilized in this study were derived from one donor. This is both good

and bad; good because it eliminated genetic variability, but bad in that the single donor may have a defective genome, and results thereof may not approximate that seen in the general population. It has been our impression over the years that some of our data variability was secondary to the use of fibroblasts from multiple donors, suggesting that some subtle genetic differences were the cause of the variability (this remains a supposition). We have opted to use fibroblasts from a single donor when performing a cluster of experiments in order to minimize the data variability. Other investigators have utilized both single [22] and multiple [23] fibroblast donors with salutary results.

The knockdown efficiency we typically obtained in the fibroblast-populated collagen matrix was modest, somewhere in the 50–75% range. We tried various measures to improve this efficiency, such as brief trypsinization prior to transfection. This technique has been shown to increase knockdown efficiency in monolayer primary human fibroblasts [16]. We confirmed that finding here, but could not extend it to the 3D collagen matrix model. We reported the monolayer result to confirm the findings of the previous investigators, and to point out that pre-transfection trypsinization is a simple method to improve the results of RNAi in difficult-to-transfect monolayer human foreskin fibroblasts. The mechanism of trypsin's effect is not clear; perhaps it is secondary to membrane trauma and transient membrane passages [24].

Given the reasonable results of knockdown in monolayer, one might propose to transfect the cells with siRNA while in monolayer, and then process these cells into collagen matrices. This would avoid the more difficult transfection with fibroblasts embedded in the collagen matrix. Indeed, transfection of monolayer human lung fibroblasts with siRNA with subsequent processing of the cells into the 3D collagen matrix already has been done, with integrin-linked kinase as the target [25]; an analogous process has been done with an adenoviral vector expressing FAK isoforms [19]. The potential problem with this sequence is that knockdown of a protein which regulates fibroblast survival (such as focal adhesion kinase [26]) while the cells are in monolayer may adversely effect the number of fibroblasts that survive the subsequent mechanical processing into collagen gels; this process involves trypsinization, multiple centrifugations, cell pellet washings, etc. That is, cells which were successfully transfected with siRNA actually may not survive the processing because the knockdown made them made them less "robust," or more "fragile." In order to avoid this (admittedly hypothetical) concern, we have been endeavoring to transfect fibroblasts which already have been embedded in the 3D collagen matrix. To date our p53 knockdown efficacy in the fibroblast-populated collagen matrix has been erratic and incomplete; the reason for this is not clear, as discussed above. Ultimately, p53 may require knockdown first in monolayer before setting up the 3D matrix.

Discussion in the literature regarding the use of proper controls in RNAi experiments is ongoing and has not achieved a resolution. Some authors have advocated the transfection of non-targeting short RNA duplex with a random sequence (i.e., "scrambled" duplex) as a negative control; however, it has been the consensus of some experts that the use of scrambled duplexes can produce misleading results and may not be helpful [27]. Other authors have advocated the transfection of short RNA duplexes with a target mismatch of 1–3 bases as a negative control; however, such sequences also can produce knockdown of the target despite the intentional sequence mismatch [28]. When we began performing RNAi experiments we employed a scrambled duplex as a negative control, and we did not observe any unexpected knockdown. We have since stopped using non-targeting short RNA duplexes as negative controls because of the controversy over their use. None of the experiments generated in this manuscript were performed with a non-targeting short RNA duplex.

In our data the degree of knockdown at the cellular level was not an "all-or-nothing" phenomenon. The immunofluorescent images suggested that a range of knockdown was occurring; some cells were virtually devoid of target, others had a high-target load, and there was a full spectrum of expression in between. It is possible that we might have been able to obtain higher and more sustained target knockdown had we employed one of the vectors which expresses siRNA in the form of shRNA (short-hairpin). The importation of large nucleotide structures into primary foreskin fibroblasts, although feasible in monolayer [19], would add yet another element of complexity if attempted in the three-dimensional collagen matrix. We therefore decided not to take this route. Although the target knockdown we obtained was not complete, it was enough to observe some biological effects, such as inhibition of cellular survival after RNAi of FAK in Fig. 6.

In regard to vector-based expression of shRNA, there also may be a greater tendency for off-target effects to occur with this technique than with straight transfection of short RNA duplexes [29]. Off-target effects have been a persistent issue with RNAi [30]; in some cases off-target effects have been shown to induce cell death [31]. Off-target effects also have been attributed to transfection vehicle toxicity, but not the formulation which we employed [32]. Recent work has demonstrated that chemical modification to the siRNA duplex (e.g., addition of side chains) can reduce off-target effects without compromising target knockdown [33]; this technology was not available when we performed our experiments.

The data of this article suggested that optimization of the transfection conditions is important for foreskin

fibroblasts, both in monolayer and in the collagen matrix. For example, there were a number of optimization experiments (not shown) that produced the result in Fig. 5A. Key variables that can influence lipoid-mediated transfection efficiency include cellular confluency, choice of proprietary formulation of transfection vehicle, concentration of the vehicle, and siRNA concentration [34]. Once inside the cell, the design/sequence of the siRNA duplex itself is important [35]. In these studies we did not carry out formal comparisons of one siRNA duplex with another, but instead relied on a mixture (pool) of four oligomers which were designed using a proprietary computational method [36, 37]. The fact that our knockdown efficiency was variable and somewhat unpredictable suggests to us that there might be some unidentified factors, such as matrix sequestration of reagents, which influence RNAi in foreskin fibroblasts.

Acknowledgments The authors would like to acknowledge the technical assistance of Chris Hansen. Supported by a grant from the NIH (K08 GM00703) to MAC. The authors also would like to thank Janice Taylor of the Confocal Laser Scanning Microscope Core Facility at the University of Nebraska Medical Center, which is supported by the Nebraska Research Initiative, for providing assistance with confocal microscopy.

References

1. Krichevsky AM, Kosik KS (2002) RNAi functions in cultured mammalian neurons. Proc Natl Acad Sci USA 99:11926–11929
2. Rubinson DA, Dillon CP, Kwiatkowski AV, Sievers C, Yang L, Kopinja J, Zhang M, McManus MT, Gertler FB, Scott ML, Van Parijs L (2003) A lentivirus-based system to functionally silence genes in primary mammalian cells, stem cells and transgenic mice by RNA interference. Nat Genet 33:401–406
3. Lattanzi L, Salvatori G, Coletta M, Sonnino C, Cusella De Angelis MG, Gioglio L, Murry CE, Kelly R, Ferrari G, Molinaro M, Crescenzi M, Mavilio F, Cossu G (1998) High efficiency myogenic conversion of human fibroblasts by adenoviral vector-mediated MyoD gene transfer. An alternative strategy for ex vivo gene therapy of primary myopathies. J Clin Invest 101:2119–2128
4. Grinnell F (1994) Fibroblasts, myofibroblasts, and wound contraction. J Cell Biol 124:401–404
5. Carlson MA, Longaker MT (2004) The fibroblast-populated collagen matrix as a model of wound healing: a review of the evidence. Wound Repair Regen 12:134–147
6. Cukierman E, Pankov R, Yamada K (2002) Cell interactions with three-dimensional matrices. Curr Opin Cell Biol 14:633–639
7. Cukierman E, Pankov R, Stevens DR, Yamada KM (2001) Taking cell-matrix adhesions to the third dimension. Science 294:1708–1712
8. Antoniades HN, Galanopoulos T, Neville-Golden J, Kiritsy CP, Lynch SE (1994) p53 expression during normal tissue regeneration in response to acute cutaneous injury in swine. J Clin Invest 93:2206–2214
9. Tyner SD, Venkatachalam S, Choi J, Jones S, Ghebranious N, Igelmann H, Lu X, Soron G, Cooper B, Brayton C, Hee Park S, Thompson T, Karsenty G, Bradley A, Donehower LA (2002) p53 mutant mice that display early ageing-associated phenotypes. Nature 415:45–53
10. Carlson MA, Longaker MT, Thompson JS (2004) Modulation of FAK, Akt, and p53 by stress release of the fibroblast-populated collagen matrix. J Surg Res 120:171–177
11. Grinnell F, Zhu M, Carlson MA, Abrams JM (1999) Release of mechanical tension triggers apoptosis of human fibroblasts in a model of regressing granulation tissue. Exp Cell Res 248: 608–619
12. Carlson MA (2006) Technical note: assay of cell quantity in the fibroblast-populated collagen matrix with a tetrazolium reagent. Eur Cell Mater 12:44–48
13. Duan WR, Garner DS, Williams SD, Funckes-Shippy CL, Spath IS, Blomme EA (2003) Comparison of immunohistochemistry for activated caspase-3 and cleaved cytokeratin 18 with the TUNEL method for quantification of apoptosis in histological sections of PC-3 subcutaneous xenografts. J Pathol 199:221–228
14. Zhu C, Wang X, Hagberg H, Blomgren K (2000) Correlation between caspase-3 activation and three different markers of DNA damage in neonatal cerebral hypoxia-ischemia. J Neurochem 75:819–829
15. Namura S, Zhu J, Fink K, Endres M, Srinivasan A, Tomaselli KJ, Yuan J, Moskowitz MA (1998) Activation and cleavage of caspase-3 in apoptosis induced by experimental cerebral ischemia. J Neurosci 18:3659–3668
16. Matheny SA, Chen C, Kortum RL, Razidlo GL, Lewis RE, White MA (2004) Ras regulates assembly of mitogenic signalling complexes through the effector protein IMP. Nature 427:256–260
17. Ilic D, Almeida EA, Schlaepfer DD, Dazin P, Aizawa S, Damsky CH (1998) Extracellular matrix survival signals transduced by focal adhesion kinase suppress p53-mediated apoptosis. J Cell Biol 143:547–560
18. Hungerford JE, Compton MT, Matter ML, Hoffstrom BG, Otey CA (1996) Inhibition of pp125FAK in cultured fibroblasts results in apoptosis. J Cell Biol 135:1383–1390
19. Xia H, Nho RS, Kahm J, Kleidon J, Henke CA (2004) Focal adhesion kinase is upstream of phosphatidylinositol 3-kinase/Akt in regulating fibroblast survival in response to contraction of type I collagen matrices via a beta 1 integrin viability signaling pathway. J Biol Chem 279:33024–33034
20. Tilghman RW, Slack-Davis JK, Sergina N, Martin KH, Iwanicki M, Hershey ED, Beggs HE, Reichardt LF, Parsons JT (2005) Focal adhesion kinase is required for the spatial organization of the leading edge in migrating cells. J Cell Sci 118:2613–2623
21. Carlson MA, Longaker MT, Thompson JS (2004) Modulation of FAK, Akt, and p53 by stress release of the fibroblast-populated collagen matrix [Erratum]. J Surg Res 121:151
22. Tian B, Lessan K, Kahm J, Kleidon J, Henke C (2002) Beta 1 integrin regulates fibroblast viability during collagen matrix contraction through a phosphatidylinositol 3-kinase/Akt/protein kinase B signaling pathway. J Biol Chem 277:24667–24675
23. Grinnell F, Ho CH, Lin YC, Skuta G (1999) Differences in the regulation of fibroblast contraction of floating versus stressed collagen matrices. J Biol Chem 274:918–923
24. Lin YC, Ho CH, Grinnell F (1997) Fibroblasts contracting collagen matrices form transient plasma membrane passages through which the cells take up fluorescein isothiocyanate-dextran and Ca2+. Mol Biol Cell 8:59–71
25. Nho RS, Xia H, Kahm J, Kleidon J, Diebold D, Henke CA (2005) Role of integrin-linked kinase in regulating phosphorylation of Akt and fibroblast survival in type I collagen matrices through a beta1 integrin viability signaling pathway. J Biol Chem 280:26630–26639
26. Parsons JT (2003) Focal adhesion kinase: the first ten years. J Cell Sci 116:1409–1416
27. (2003) Whither RNAi? Nat Cell Biol 5:489–490
28. Saxena S, Jonsson ZO, Dutta A (2003) Small RNAs with imperfect match to endogenous mRNA repress translation.

Implications for off-target activity of small inhibitory RNA in mammalian cells. J Biol Chem 278:44312–44319
29. Scherr M, Eder M (2004) RNAi in functional genomics. Curr Opin Mol Ther 6:129–135
30. Jackson AL, Linsley PS (2004) Noise amidst the silence: off-target effects of siRNAs? Trends Genet 20:521–524
31. Fedorov Y, Anderson EM, Birmingham A, Reynolds A, Karpilow J, Robinson K, Leake D, Marshall WS, Khvorova A (2006) Off-target effects by siRNA can induce toxic phenotype. RNA 12:1188–1196
32. Fedorov Y, King A, Anderson E, Karpilow J, Ilsley D, Marshall W, Khvorova A (2005) Different delivery methods-different expression profiles. Nat Methods 2:241
33. Jackson AL, Burchard J, Leake D, Reynolds A, Schelter J, Guo J, Johnson JM, Lim L, Karpilow J, Nichols K, Marshall W, Khvorova A, Linsley PS (2006) Position-specific chemical modification of siRNAs reduces "off-target" transcript silencing. RNA 12:1197–1205
34. Sambrook J, Russell DW (2001) Molecular cloning: a laboratory manual. Cold Spring Harbor Laboratory Press, Cold Spring Harbor
35. Mittal V (2004) Improving the efficiency of RNA interference in mammals. Nat Rev Genet 5:355–365
36. Boese Q, Leake D, Reynolds A, Read S, Scaringe SA, Marshall WS, Khvorova A (2005) Mechanistic insights aid computational short interfering RNA design. Methods Enzymol 392:73–96
37. Reynolds A, Leake D, Boese Q, Scaringe S, Marshall WS, Khvorova A (2004) Rational siRNA design for RNA interference. Nat Biotechnol 22:326–330